Proposed High-Current rf Linear Accelerators with Beams in Thermal Equilibrium

Martin Reiser and Nathan Brown
Institute for Plasma Research, Electrical Engineering and Physics Departments, University of Maryland, College Park, Maryland 20742
(Received 19 September 1994)

In the conventional design of rf linear accelerators (linacs) the charged-particle bunches are not in three-dimensional thermal equilibrium. For applications requiring high beam currents, the space charge couples the longitudinal and transverse particle motions. This leads to equipartitioning processes which cause unacceptable emittance growth and halo formation. A new design strategy for high-current rf linacs is proposed in which the bunches are in thermal equilibrium so that these effects do not occur. Analytic relationships and scaling laws for the design of such linacs are presented.

PACS numbers: 41.85.Ew, 29.17.+w, 52.25.Wz

Many advanced applications of rf linear accelerators, such as injector linacs for high-energy physics colliders, spallation neutron sources, transmutation of radioactive nuclear waste, heavy-ion inertial fusion, and free electron lasers, require high beam currents where space charge effects play a dominant role in the beam physics. In the conventional design of such linacs the bunched beams are not in thermal equilibrium (see Ref. [1], Appendix 4). Space-charge forces couple the longitudinal and transverse motions and drive the beam towards an equipartitioned state causing significant emittance growth and hence beam quality deterioration, as was first demonstrated by Jameson in computer simulation studies [2]. Hofmann [3] analyzed beams having 2D anisotropic temperature distributions and found that collective instabilities with distinct thresholds occur due to resonant-type interaction of the forces in the two degrees of freedom (e.g., coupling of the longitudinal and transverse motion). Jameson, in his very extensive computer simulation work [2,4], confirmed Hofmann's predictions and tried to develop rf linac designs which minimize the effects of instabilities and the associated emittance growth. His simulation results, as well as the recent studies by Wangler *et al.* [5], show conclusively that no emittance growth occurs if the beam is equipartitioned. This is in agreement with Hofmann's analysis and the general thermodynamic principle that thermal equilibrium is a state of minimum energy.

Of particular concern for linacs with high average power is the formation of halos and the associated beam loss due to equipartitioning and beam mismatch that may cause excessive nuclear activation and prevent "hands-on" maintenance of the machines (losses must remain below 1 nA/m). Such halos have been observed in existing high-current linacs like LAMPF [6] and in recent experiments with mismatched beams at the University of Maryland [7]. Halo formation is an important topic of on-going theoretical research [8–10].

In Ref. [1], the theoretical framework for a self-consistent description of bunched beams, the causes of equipartitioning, and the design strategy for an equilibrated beam in rf linacs was developed. When coupling due to space charge is weak or negligible, the beam can be in a metaequilibrium state with different transverse and longitudinal temperatures $T_\perp$ and $T_\parallel$, respectively [11]. However, when space-charge coupling forces are significant, the two-temperature distribution is not a solution to the steady-state Vlasov equation and is therefore intrinsically unstable. This is the cause of the equipartitioning effect which drives bunched beams toward thermal equilibrium. The thermal-equilibrium properties of bunched beams, including the effects of images [12], is being examined in a separate paper by the authors [13]. In this Letter, we present the results of new analytic work on equipartitioned beams in rf linacs which is based on the theoretical description of bunched beams in Ref. [1].

We start with the coupled fourth-order envelope equations [(5.502) and (5.503) of Ref. [1]] for a short bunch where image effects are negligible, which are repeated here for easy reference:

$$k_{x0}^2 a - \frac{3}{2}\frac{Nr_c}{\beta_0^2\gamma_0^3}\frac{1}{az_m}\left(1 - \frac{1}{3}\frac{a}{\gamma_0 z_m}\right) - \frac{\epsilon_{nx}^2}{\beta_0^2\gamma_0^2 a^3} = 0, \tag{1}$$

$$k_{z0}^2 z_m - \frac{Nr_c}{\beta_0^2\gamma_0^4}\frac{1}{az_m} - \frac{\epsilon_{nz}^2}{\beta_0^2\gamma_0^6 z_m^3} = 0. \tag{2}$$

The applied transverse and longitudinal focusing forces acting on the particles are represented, respectively, by the wave numbers

$$k_{x0} = \frac{\sigma_{x0}}{n\beta_0\lambda}, \tag{3}$$

$$k_{z0} = \left(-\frac{2\pi q E_m \sin\varphi_0}{\lambda mc^2\beta_0^3\gamma_0^3}\right)^{1/2}. \tag{4}$$

Here, σ_{x0} is the phase advance of the transverse "betatron" oscillations per focusing period of length $n\beta_0\lambda$ (where n is an integer ≥ 2), E_m is the accelerating electric

0031-9007/95/74(7)/1111(4)$06.00 © 1995 The American Physical Society

field gradient, $\varphi_0 < 0$ is the phase of the synchronous particle (bunch centroid), $\beta_0 = v_0/c$ and $\gamma_0 = (1 - \beta_0^2)^{-1/2}$ are the relativistic velocity and energy factors, v_0 is the centroid velocity, c is the speed of light, q is the particle charge, m is the particle mass, and λ is the wavelength of the rf field in the accelerating structure of the rf linac. N is the number of particles in the bunch, related to the average beam current $\bar{I}$ by $N = \bar{I}\lambda/qc$, $r_c = q^2/4\pi\epsilon_0 mc^2$ is the classical particle radius, and ϵ_0 is the permittivity of free space. ϵ_{nx} and ϵ_{nz} are the normalized transverse and longitudinal emittances, a and z_m are the peak radius and half length of the "equivalent" uniform-density ellipsoidal bunch that is used here to model the nonanalytic Boltzmann distribution with the same second moments or rms widths, $\tilde{x}$, $\tilde{z}$, and emittances, $\tilde{\epsilon}_{nx}$, $\tilde{\epsilon}_{nz}$ (for the ellipsoidal bunch one has $a = \sqrt{5}\,\tilde{x}$, $z_m = \sqrt{5}\,\tilde{x}$, $\epsilon_{nx} = 5\tilde{\epsilon}_{nx}$, and $\epsilon_{nz} = 5\tilde{\epsilon}_{nz}$).

From the definitions of the transverse and longitudinal rms emittances, $\tilde{\epsilon}_{nx} = \tilde{x}(\gamma_0 k_B T_\perp/mc^2)^{1/2}$ and $\tilde{\epsilon}_{nz} = \tilde{z}(\gamma_0^3 k_B T_\parallel/mc^2)^{1/2}$ [Ref. [1], Eqs. (5.290b) and (5.317b)], the condition for the beam to be equipartitioned is [Ref. [1], Eq. (A.4.6)]

$$\frac{\epsilon_{nx}}{\epsilon_{nz}}\,\frac{\gamma_0 z_m}{a} = 1\,. \tag{5}$$

The envelope equations (1) and (2) and the analytic relations derived from them are valid approximations only for short bunches with aspect ratios of $0.7 < \gamma_0 z_m/a \leq 4$, which for equipartitioned beams imply emittance ratios in the same range, i.e., $0.7 < \epsilon_{nz}/\epsilon_{nx} \leq 4$, in view of Eq. (5). By substituting the equipartitioning condition (5) into the envelope equations (1) and (2), we obtain for the ratio of the focusing wave numbers for an equipartitioned beam the relation

$$\frac{k_{x0}}{k_{z0}} = \left[\frac{\frac{3}{2}(Nr_c a/\epsilon_{nx}^2)\epsilon_{nz}/\epsilon_{nx} - \frac{1}{2}Nr_c a/\epsilon_{nx}^2 + \epsilon_{nz}^2/\epsilon_{nx}^2}{Nr_c a/\epsilon_{nx}^2 + 1}\right]^{1/2}, \tag{6}$$

which depends in general on the emittance ratio, $\epsilon_{nz}/\epsilon_{nx}$, and on the intensity parameter

$$\frac{Nr_c a}{\epsilon_{nx}^2} = \frac{\bar{I}}{I_0}\,\frac{\lambda a}{\epsilon_{nx}^2}\,, \tag{7}$$

where $I_0 = 4\pi\epsilon_0 mc^3/q$. The relationship between k_{x0}/k_{z0} and $\epsilon_{nz}/\epsilon_{nx}$ is plotted in Fig. 1 for different values of the intensity parameter. Equation (6) shows that in an equipartitioned linac the ratio of the two focusing wave numbers is uniquely determined. The traditional choice of constant σ_{x0} (i.e., $k_{x0} \propto 1/\beta_0$) and constant $E_m|\sin\varphi_0|$, so that $k_{x0}/k_{z0} \propto \beta_0^{1/2}\gamma_0^{3/2}$, increases the temperature anisotropy $T_\perp/T_\parallel$ and the aspect ratio $\gamma_0 z_m/a$ during acceleration and is responsible for the equipartitioning effect and associated emittance growth in conventional high-current machines.

For a space-charge dominated beam, where $Nr_c a/\epsilon_{nx}^2 \gg 1$, we obtain from (6) the solution

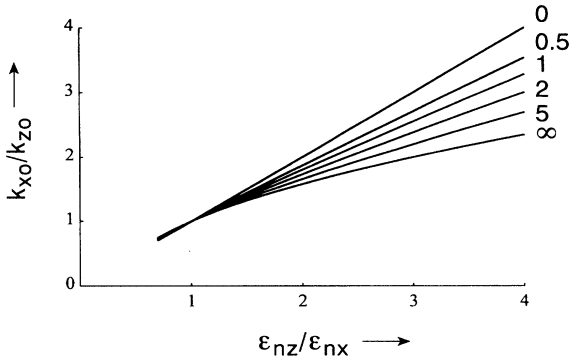

FIG. 1. The ratio of the focusing wave numbers (k_{x0}/k_{z0}) as a function of the ratio of the emittances ($\epsilon_{nz}/\epsilon_{nx}$) from Eq. (6) for several values of the intensity parameter ($Nr_c a/\epsilon_{nx}^2 = 0$, 0.5, 1, 2, 5, and ∞).

$$\frac{k_{x0}}{k_{z0}} = \left(\frac{3}{2}\,\frac{\epsilon_{nz}}{\epsilon_{nx}} - \frac{1}{2}\right)^{1/2}, \tag{8}$$

which is identical to Eq. (A4.12) of Ref. [1]. In this regime, the focusing ratio k_{x0}/k_{z0} is practically independent of the beam intensity, which greatly simplifies the design calculations.

By using the relation (5) in the envelope equations (1) and (2) and our approximation to a fourth-order polynomial [14] we find for the radius and half length of the bunch in an equipartitioned rf linac the approximate solutions

$$a \approx \left[\frac{3}{2}\,\frac{Nr_c}{\beta_0^2\gamma_0^2}\,\frac{1}{k_{z0}^2}\,\frac{\epsilon_{nx}}{\epsilon_{nz}}\left(1 - \frac{1}{3}\,\frac{\epsilon_{nx}}{\epsilon_{nz}}\right) + \left(\frac{\epsilon_{nx}}{\beta_0\gamma_0 k_{x0}}\right)^{3/2}\right]^{1/3}, \tag{9}$$

$$z_m \approx \left[\frac{Nr_c}{\beta_0^2\gamma_0^5}\,\frac{1}{k_{z0}^2}\,\frac{\epsilon_{nz}}{\epsilon_{nx}} + \left(\frac{\epsilon_{nz}}{\beta_0^2\gamma_0^3 k_{z0}}\right)^{3/2}\right]^{1/3}, \tag{10}$$

The most important parameters in rf linac design are the rf wavelength λ, the bunch radius a and the electric field gradient E_m, or k_{z0}. The radius must be significantly smaller than the drift tube radius b (i.e., $a/b \ll 1$), and for geometrical reasons both a and b are proportional to λ. The gradient E_m also depends on λ, being limited either by high voltage breakdown or by cost considerations (power dissipation in the conducting walls). For a high-power, light-ion accelerator (e.g., p, H^-, d), which will be used here as an example, we have the scaling

$$a \propto \lambda, \qquad E_m \propto (1/\lambda)^{1/2}. \tag{11}$$

With this dependence is mind, we use the substitution $z_m = (a/\gamma_0)\epsilon_{nz}/\epsilon_{nx}$ from (5) to obtain from (10) an equation for the radius in terms of k_{z0} rather than k_{x0}, namely

$$a \approx \left[\frac{Nr_c}{\beta_0^2\gamma_0^2}\left(\frac{\epsilon_{nx}}{\epsilon_{nz}}\right)^2\frac{1}{k_{z0}^2} + \left(\frac{\epsilon_{nx}}{\epsilon_{nz}}\right)^3\left(\frac{\epsilon_{nx}}{\beta_0\gamma_0 k_{z0}}\right)^{3/2}\right]^{1/3}. \tag{12}$$

We can solve this equation for the particle number N, or alternatively for the average current $\bar{I} = qNc/\lambda$, and obtain

$$\bar{I} = I_0 \frac{a^3}{\lambda} \beta_0^2 \gamma_0^2 k_{z0}^2 \left(\frac{\epsilon_{nz}}{\epsilon_{nx}}\right)^2 \left[1 - \left(\frac{\epsilon_{nx}^2}{\epsilon_{nz}} \frac{1}{\beta_0 \gamma_0 k_{z0}}\right)^{3/2} \frac{1}{a^3}\right]. \tag{13}$$

At the space-charge limit, where the emittance term in the bracket is zero, the average current has a maximum $\bar{I}_{\max}$. Substituting from (4) for k_{z0} we find

$$\bar{I}_{\max} = I_0 \frac{a^3}{\lambda^2} \frac{2\pi q E_m |\sin\varphi_0|}{mc^2 \beta_0 \gamma_0} \left(\frac{\epsilon_{nz}}{\epsilon_{nx}}\right)^2 = \frac{\pi}{15} \frac{a^3}{\lambda^2} \frac{E_m |\sin\varphi_0|}{\beta_0 \gamma_0} \left(\frac{\epsilon_{nz}}{\epsilon_{nx}}\right)^2. \tag{14}$$

In view of (11) we see that the maximum current in an equipartitioned beam is proportional to $(\lambda^{1/2}/\beta_0\gamma_0)(\epsilon_{nz}/\epsilon_{nx})^2$. It follows that the lower limit for $\bar{I}_{\max}$ occurs at the high-energy, high-frequency (low-wavelength) end of the accelerator system and not at the low-energy end (front part) as in the conventional, nonequipartitioned linac design.

The set of equations (5), (6), and (12), together with relation (4) for k_{z0}^2, can be used to design an rf linac with an equipartitioned beam for given particle number N (or average current $\bar{I}$), normalized emittances, $\epsilon_{nx}, \epsilon_{nz}$, final energy or $(\beta_0\gamma_0)_{\max}$, and synchronous phase φ_0. The wavelength λ and field gradient E_m at full energy are chosen to obtain from (12) a value of the radius a that assures the desired clearance between the beam edge and the tube radius b. The gradient E_m, which determines k_{z0}, is usually constant in each structure, with $E_m(\lambda_2) = (\lambda_1/\lambda_2)^{1/2} E_m(\lambda_1)$ if a transition is made from a low-frequency structure with wavelength λ_1 to a high-frequency structure with wavelength λ_2. The variation of transverse focusing (k_{x0}) with energy is determined from Eq. (6); the corresponding phase advance σ_{x0} can be calculated from Eq. (3). The half length z_m of the bunch, or alternatively the phase width $\Delta\varphi_m = 2\pi z_m/\beta_0\lambda$, is calculated from Eqs. (5) or (10).

As an example, let us consider the equipartitioned proton linac discussed in Ref. [1], Appendix 4 and in Refs. [15] and [16]. It has average current $\bar{I} = 100$ mA, kinetic energy varying from 2 MeV ($\gamma_0 = 1$, $\beta_0 = 0.065$) to 938 MeV ($\gamma_0 = 2$, $\beta_0 = 0.866$), emittances $\epsilon_{nx} = 6.85 \times 10^{-7}$ m rad and $\epsilon_{nz} = 2\epsilon_{nx}$, $\varphi_0 = -40°$, frequency 200 MHz ($\lambda = 1.5$ m) and gradient $E_m = 1.6$ MV/m at low energy, 800 MHz ($\lambda = 0.375$ m) and 3.2 MV/m at high energy. The transition from the 200 to the 800 MHz structure occurs at the energy of 22 MeV and is defined by the condition that the radius a at the end of the 200 MHz linac is the same as at full energy (938 MeV, 800 MHz). In the 800 MHz structure only every fourth rf bucket is occupied so that the average current (100 mA) is one-fourth of the theoretical limit given in Eq. (13). From the above equations we obtain for the bunch size the following results: at 2 MeV, $a \approx 2.65$ mm, $z_m = 2a = 5.3$ mm, and $\Delta\varphi_m = 19.6°$; at 938 MeV, $a = z_m \approx 3.9$ mm and $\Delta\varphi_m = 4.3°$.

These numbers are well within the practical design considerations of a high-current rf linac. The bunch radius at high energy is larger than in the conventional linac design, but the density profile is sharp-edged, as illustrated in Fig. 2, and does not exhibit the long Gaussian tail of beams with stronger radial focusing in existing linacs. Figure 3 shows the transverse and longitudinal space-charge tune depressions, respectively, k_x/k_{x0} and k_z/k_{z0}, and the peak ellipsoidal radius in units of its maximum value at 938 MeV, all as functions of the energy. The sharp changes in the curves indicate the increase of the focusing strengths and the resulting decrease of the bunch radius after transition to the 800 MHz structure at 22 MeV. Here, k_x and k_z are, respectively, the transverse and longitudinal focusing wave numbers with space charge, and the tune depressions are calculated from Eqs. (1) and (2):

$$\frac{k_x}{k_{x0}} = \left(1 - \frac{3Nr_c(1 - a/3\gamma_0 z_m)}{2\beta_0^2\gamma_0^3 a^2 z_m k_{x0}^2}\right)^{1/2}, \tag{15}$$

$$\frac{k_z}{k_{z0}} = \left(1 - \frac{Nr_c}{\beta_0^2\gamma_0^4 z_m^2 a k_{z0}^2}\right)^{1/2}. \tag{16}$$

In future high-current superconducting rf linacs [17,18] the electric field gradients and the drift-tube bore radii could be increased significantly so that smaller bunch sizes and larger values for the clearance ratio b/a could be achieved. Thus, since for a space-charge dominated beam $a \propto E_m^{-1/3}$ [from (4) and (12)], increasing E_m from 3.2 to 9.6 MV/m in our above example would decrease the final radius from 3.9 to $a \approx 2.6$ mm.

The main advantage of the design strategy presented here is that the beam is in thermal equilibrium, i.e., in a stable state of minimum energy where ideally no

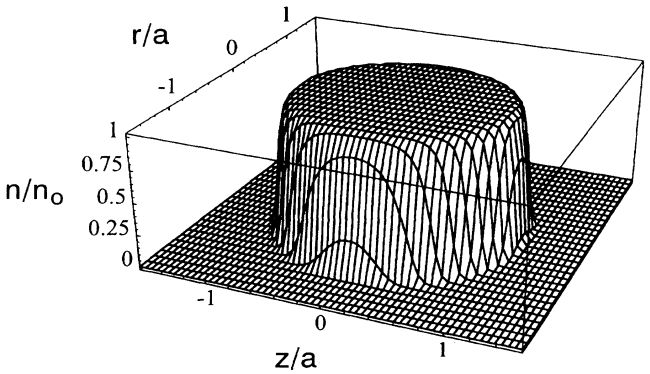

FIG. 2. Density profile for the thermal equilibrium distribution at 938 MeV in the example of the 100 mA proton linac. Distances and density are in units of the radius and density, respectively, of the equivalent uniform ellipsoid. The pipe is located at $b = 2$ cm ($\approx 5a$) and does not have a significant effect on the distribution.

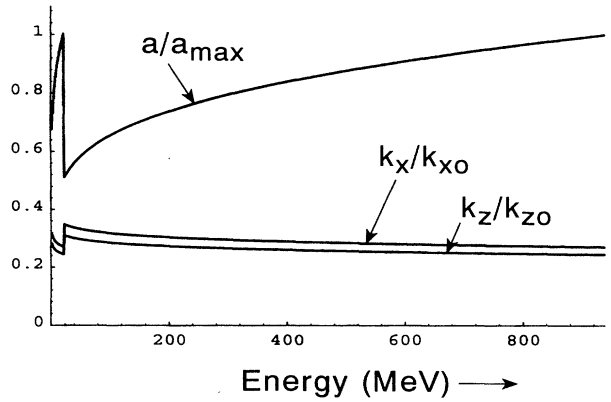

FIG. 3. Three beam parameters as functions of the energy for the 100 mA proton linac: the peak radius obtained from Eq. (9) divided by its maximum value (a_{max} of 3.9 mm at 938 MeV), and the transverse and longitudinal space-charge tune depressions, calculated from Eqs. (15) and (16). The sharp changes in the curves occur at the transition from the 200 to the 800 MHz structure at 22 MeV.

emittance growth or halo formation should occur. In practice, there will always be deviations from the ideal equilibrium state due to beam mismatch, misalignments, and other imperfections. However, the emittance growth resulting from such effects will always be less than in the conventional design where equipartitioning adds significantly to the overall emittance increase and halo formation.

This work is supported by the U.S. Department of Energy.

[1] M. Reiser, *Theory and Design of Charged Particle Beams* (John Wiley & Sons, New York, 1994).
[2] R. A. Jameson, IEEE Trans. Nucl. Sci. **NS-28**, 2408 (1981).
[3] I. Hofmann, IEEE Trans. Nucl. Sci. **NS-28**, 2399 (1981).
[4] R. A. Jameson, in *Advanced Accelerator Concepts,* edited by J. S. Wurtele, AIP Conf. Proc. No. 279 (AIP, New York, 1993).
[5] T. P. Wangler, T. S. Bhatia, G. H. Neuschaefer, and M. Pabst, "Conference Record of the 1989 IEEE Particle Accelerator Conference," Report No. 89CH2669-0, March 1989, p. 1748.
[6] R. A. Jameson (private communication).
[7] D. Kehne, M. Reiser, and H. Rudd, "Conference Record of the IEEE 1993 Particle Accelerator Conference," Report No. 93CH3279-7, p. 65; see also M. Reiser, *Theory and Design of Charged Particle Beams* (Ref. [1], Section 6.2.2); M. Reiser, J. Appl. Phys. **70**, 1919 (1991).
[8] R. A. Jameson, Los Alamos National Laboratory Report No. LA-UR-93-1209, March 1993, and references therein.
[9] R. L. Gluckstern, Phys. Rev. Lett. **73**, 1247 (1994).
[10] J. M. Lagniel, Nucl. Instrum. Methods Phys. Res., Sect. A **345**, 46 (1994).
[11] M. Reiser and N. Brown, Phys. Rev. Lett. **71**, 2911 (1993).
[12] C. K. Allen, N. Brown, and M. Reiser, Part. Accel. **45**, 149 (1994); see also M. Reiser, *Theory and Design of Charged Particle Beams* (Ref. [1], Section 5.4.7).
[13] N. Brown and M. Reiser, "Thermal Equilibrium of Bunched Charged Particle Beams" (to be published).
[14] N. Brown and M. Reiser, Part. Accel. **43**, 231 (1994).
[15] M. Reiser, in Proceedings of the International Conference on Accelerator-Driven Transmutation Technologies and Applications, Las Vegas, July 1994 (unpublished).
[16] M. Reiser, in Proceedings of the 17th International Linac Conference, Tsukuba, Japan, August 1994 (unpublished).
[17] J. R. Delayen, C. L. Bohn, and C. T. Roche, Nucl. Instrum. Methods Phys. Res., Sect. B **56/57**, 1025 (1991).
[18] T. P. Wangler *et al.,* in "Conference Record of the IEEE 1993 Particle Accelerator Conference," Report No. 93CH3279-7, p. 1715; J. R. Delayen *et al., ibid.*, p. 1712.